VALIDATION OF CFD FOR CONTAINMENT JET FLOWS INCLUDING CONDENSATION

Matthias Heitsch, Daniele Baraldi, Heinz Wilkening

JRC, Institute for Energy, Postbus 2, NL-1755 ZG Petten, Netherland

Matthias.Heitsch@ec.europa.eu

Tel: 0031 224 56 5162

Abstract

The advanced validation of a CFD code for containment applications requires the investigation of water steam in the different flow types like jets or buoyant plumes.

This paper addresses therefore the simulation of two "HYJET" experiments from the former Battelle Model Containment by CFX. These experiments involve jet releases into the multi-compartment geometry of the test facility accompanied by condensation of steam at walls and in the bulk gas. In both experiments mixtures of helium and steam are injected. Helium is used to simulate hydrogen. One experiment represents a fast jet whereas in the second test a slow helium-steam release is investigated. CFX was earlier extended by bulk and wall condensation models and is able to model all relevant phenomena observed during the experiments. The paper focuses on the simulation of the two experiments employing an identical model set-up. This provides information on how well a wider range of flowing conditions in case of a full containment simulation can be covered. Some aspects related to numerical and modelling uncertainties of CFD calculations are included in the paper by investigating different turbulence models together with the modelling errors of the differencing schemes applied.

1 INTRODUCTION

During a severe accident the combined release of hydrogen and steam into the containment of a nuclear power plant is likely. Whereas close to the release location a critical or sub-critical jet develops, in the far-field often nearly stagnant flow conditions can be found. This combination of flow conditions is crucial for a realistic simulation of an accident scenario. The steam fraction of a multi-component jet is affected by the lower temperature of the surrounding atmosphere and the cold solid structures in the containment. This leads to condensation in the bulk flow and on walls. All these aspects were investigated in a series of experiments at the Battelle Model Containment (BM-C) called HYJET (Kanzleiter, 1996). Two selected tests of HYJET are simulated in this work. Earlier, a pure helium-in-air experiment from this family of tests was already simulated (Heitsch, 2000 and Wilkening, 2008). One of the current experiments represents a slow vertical helium-steam jet with a nominal release speed of about 4.9 m/s. The second test addresses a much higher jet speed of approximately 730 m/s. As a result of the simulation of both experiments more confidence in the selection of the right turbulence model for containment mixing analyses (Heitsch, 2007) and additional information about the applied condensation model are expected.

1.1 Test Facility

The Battelle Model Containment was a complex large-scale test facility (dismantled in 1999) which was used in many test series investigating containment specific phenomena. It is built from concrete and consists of many interconnected compartments. The walls have steel liners. The total inner volume sums up to about 600 m^3. The total height of the facility is about 9 m. The height of the individual

compartments inside the BM-C is in the order of 2 m. Some of the compartments are curved others are cylindrical. A vertical cut through the facility is depicted in Fig. 1. This figure shows several main compartments together with some flow connections which are relevant for the experiments under consideration. Another impression of the spatial shape and the curvature of many compartments can be seen in the computer model of the facility in Fig. 5.

Due to earlier experiments which included hydrogen deflagrations and tests at increased pressure a small leakage rate from the BM-C exists. But this leakage is not relevant for the experiments investigated here because they do not create high pressures and have a comparably short duration.

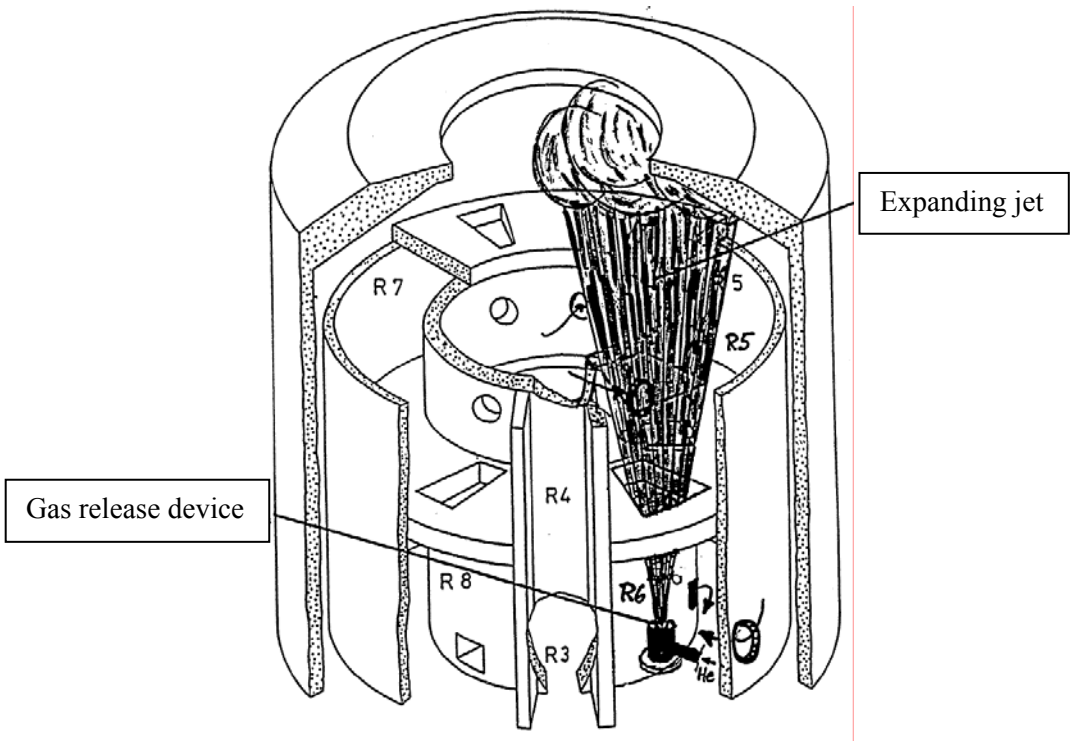

Fig. 1 Vertical cut through the Battelle Model Containment (B-MC), (Kanzleiter, 1996)

In order to minimize the interaction of the helium jet with the surrounding walls of the compartments the gas release during the HYJET experiments was located such that the jet could pass vertically through a sequence of rooms and openings. A vertical cut through the given arrangement is shown in Fig. 2. The flow release device itself (left part of Fig. 2) consists of an internal mixing section with a perforated large pipe and a mixing sheet above. Several plates with different opening diameters form the upper end of the mixing chamber. By removing or placing these plates a wide range of jet release speeds can be achieved. All flows entering the model containment have to pass through the mixing chamber. The dotted red line in Fig. 2 denotes the lower boundary of the computational model within the gas release chamber. At this elevation an ideally mixed gas flow with a flat velocity profile is assumed.

The mixture of helium and steam is prepared outside of the mixing chamber. When flowing through the mixing device, the helium fraction of the mixture is warmed up to the steam temperature. Together with heat losses to the walls of the mixing device some uncertainty about the real steam mass fraction passing through the injection opening exists because all measurements were done at the individual mixing components prior to mixing.

The measurement system of the BM-C consists mainly of thermocouples, helium sensors and flow meters. No steam concentration measurements are available. The about 70 thermocouples are of the type Ni-CrNi with a diameter of 1.5 mm and an uncertainty range of ±1.4 K. Helium concentrations are measured based on heat conduction differences with an accuracy of about ±0.5 Vol-%. Flow speeds are based on turbine flow meters in flow openings and can provide averaged measurements with an uncertainty of ±0.2 m/s. Transient helium volume fractions were recorded mainly inside the jet region as shown in Fig. 2 (all sensors starting with JKP) and at selected positions outside of it. Temperature sensors were located in the jet region (sensors JTL) together with the helium probes but also outside of this region to monitor the gas and wall structure temperature development.

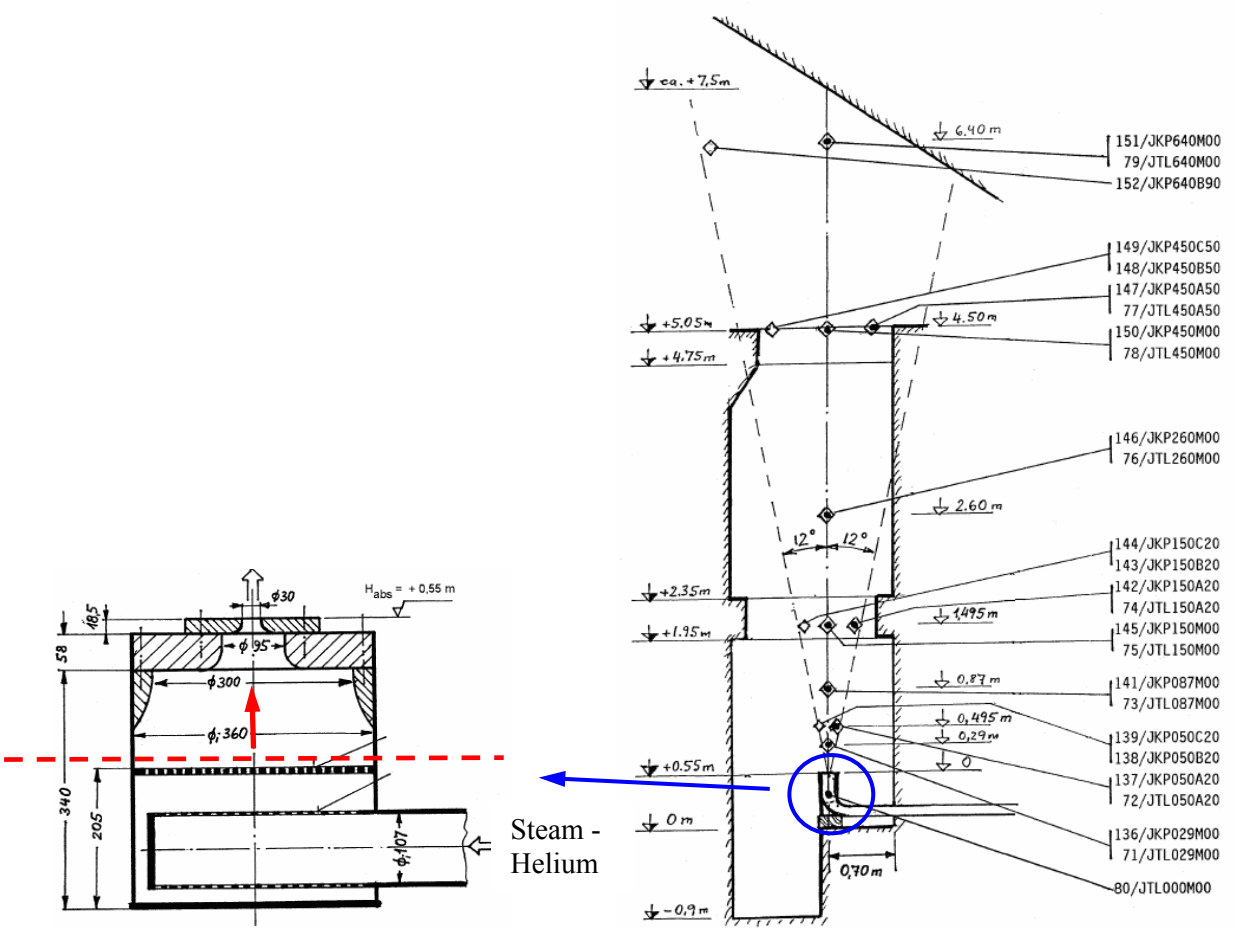

Fig. 2 Gas release chamber and distribution of probes along the jet axis

Apart from the jet itself in many compartments of the test facility very low or almost stagnant flow conditions were found during the HYJET experiments. Flow measurement was therefore restricted to the flow openings between the compartments through which a directed one-dimensional flow can be expected. In this work, a selection of flow openings is used for comparison with the simulations. Fig. 3 shows all flow paths which were opened up during the HYJET experiments together with the names of those openings selected for comparisons. An important opening is U69 which is very close to the gas release device. This opening would create an unsymmetrical air entrainment into the jet and a displacement of the jet axis. Consequently, a reflecting plate was put in front of this opening to reduce the entrainment effect as much as possible. The plate can be seen in Fig. 3 and more closely in Fig. 5.

Vertical flows as through U59B are aligned with one of the axes in the simulation model. In these cases the respective velocity component from the code simulation contains all the information needed

for comparison. A principal difficulty in performing comparisons for horizontal flows appeared. These openings, however, are not in parallel to one of the coordinate axes. For these flows the rooted mean square of the velocity components can be used as the total speed but the direction is lost. As long as there is no flow reversal during the experiment no problem occurs. A change in the flow direction however is not reflected in the results.

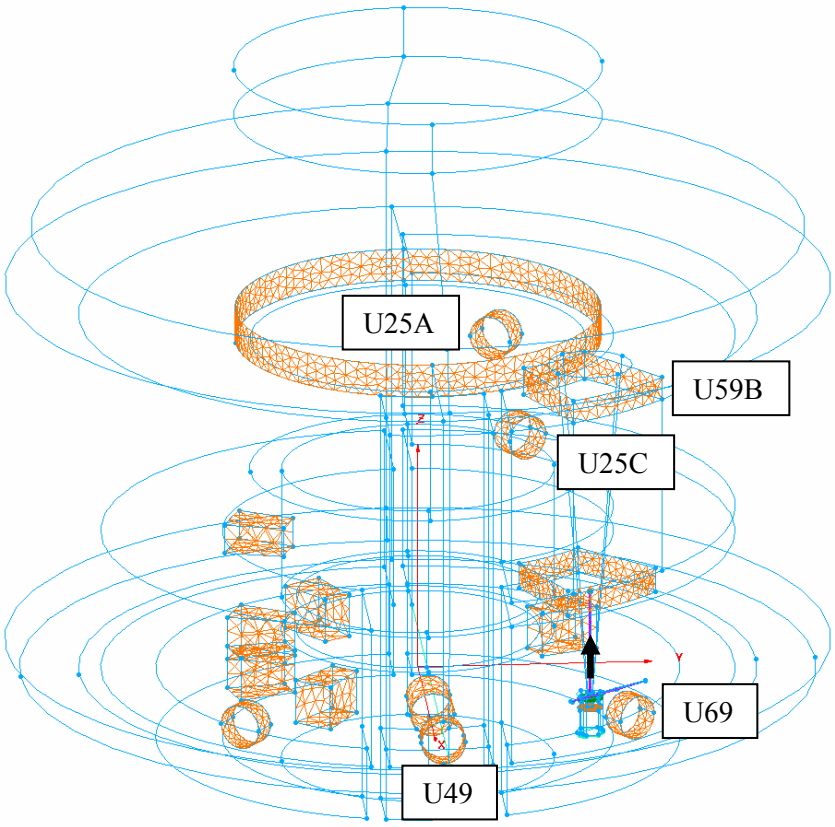

Fig. 3 Available flow openings between compartments (named openings are used for comparison with measurements)

Both experiments under investigation were carried out by heating up the whole test facility over hours before the helium injection was activated. In the heating-up phase steam with the same parameters as being used for the experiments was blown into the test facility. Short before the start of helium injection a thermal equilibrium in the gas space of the model containment close to a steady state could be achieved. The concrete structures were also warmed up sufficiently to maintain constant wall temperatures during the experiments. At the end of the heating phase there was still a vertical stratification of room and wall temperatures but this could be taken into account in the simulations as initial condition. More discussion is found in paragraph 2.2. During the injection of helium the steam flow was maintained, thus establishing a helium-steam mixture flowing into the saturated air-steam atmosphere of the test facility.

1.2 Slow Jet Experiment (Jx4)

This experiment with the internal name Jx4 investigated a slow buoyant jet with a nominal pipe outlet speed of about 4.9 m/s. The pipe outlet diameter chosen for this test was 95 mm. The injection of helium lasted approximately 490 s. A total of 1.05 kg helium was added during this time to the BM-C. The steam injection which was used before the test to pre-heat the facility continued during the helium phase. The volume fraction of helium at the inflow opening to the model containment was consequently slightly above 73 %.

1.3 Fast Jet Experiment (Jx81)

The high speed experiment Jx81 included an injection speed of about 730 m/s. This was achieved by increasing the incoming mass flow and using a pipe outlet diameter of 30 mm from the mixing chamber. The flow rates of steam and helium are much higher compared with the previous experiment. The injection time was limited to 215 s. During this time about 8.1 kg helium were injected. The composition of the total flow was similar to test Jx4 but the helium volume fraction was slightly lower at around 61 %.

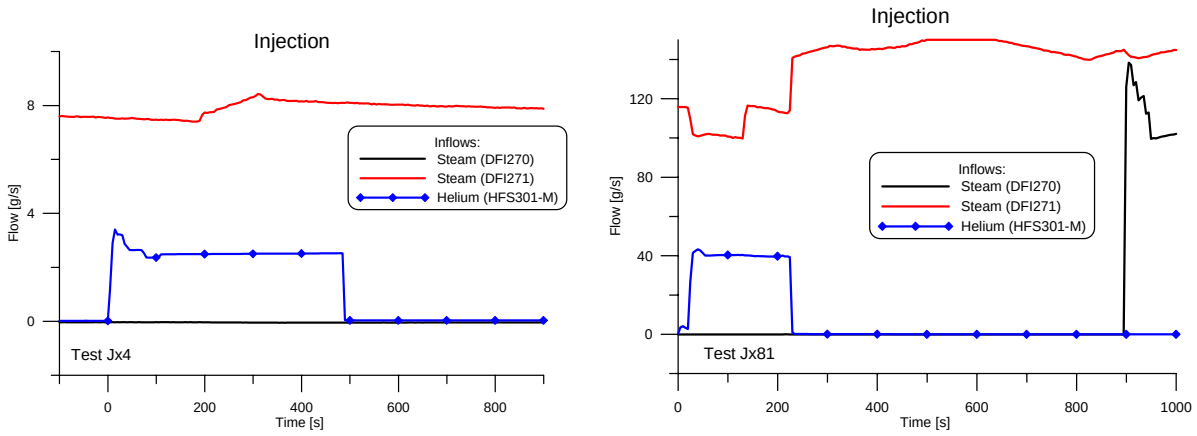

Fig. 4 Flow rates of steam and helium for test Jx4 (left) and Jx81 (right)

Fig. 4 represents the flow histories of both experiments. The steam flow is not interrupted during the helium injection phase. In principle there were two contributions to the total steam flow but during the tests only one was active. The mass flows are very different for the two experiments in order to establish the jet release speeds of 4.9 and 730 m/s respectively.

2 COMPUTATIONAL MODEL

Previous validation activities (e.g. Andreani, 2006) employing best practice guidelines and numerous investigations on the mesh sensitivity of numerical results provided experience how to create a grid to keep mesh sensitivity at a low level. This experience involves a sufficient number of cells over the cross section of openings, close to walls and a high resolution along the flow path of a jet. These requirements sometimes need compromises if the problem time to be covered is very long as for full containment applications. The formation of the grid of the BM-C is not affected because the simulation times (800 s) are short.

2.1 Mesh

The grid created to simulate the two helium-steam experiments includes all the compartments and flow openings of the BM-C involved in the tests. An overview together with the average cell size and cell density on surfaces outside the jet region is given in Fig. 5.

Fig. 5 also includes a close-up of the mixing device though which the mixture of helium and steam has to pass before it is released into compartment R6 of the test facility. Close to the mixing device there is opening U69. As already discussed a metal sheet was placed in front of U69 to limit the asymmetrical entrainment of gas through this opening.

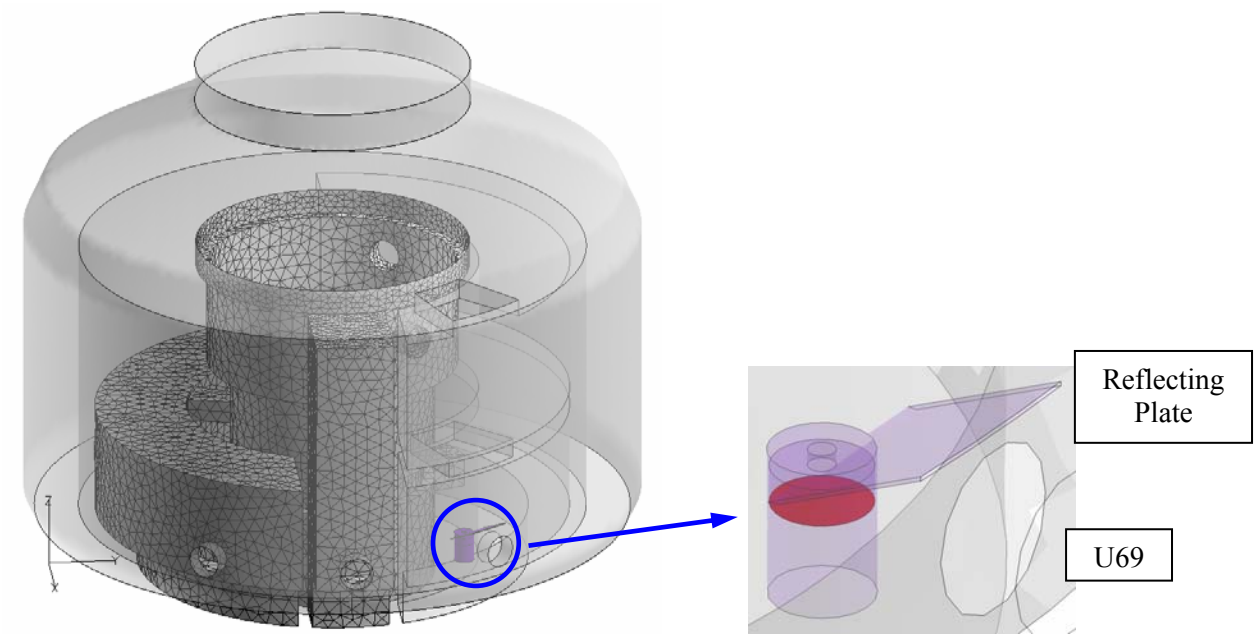

Fig. 5 Model of the test facility and a close-up of the release section

First simulations were carried out with the release direct at the pipe opening with the correct diameter for the respective experiment. The mixing chamber was completely excluded from the mesh. A flat outflow profile had to be assumed because of lack of other information. Later, a remarkable improvement of the simulation results along the jet axis could be obtained when the mixing chamber was included in the numerical mesh. The red area in Fig. 5 was defined as the release location for all the simulations discussed here. This simulation method is very close to the real situation in the test facility. Now the velocity profile at the release opening from the mixing chamber is stronger concentrated towards the central axis and is not flat anymore. The improvement obtained in the prediction of the helium concentration closest to the outlet from the mixing device is illustrated in Fig. 6.

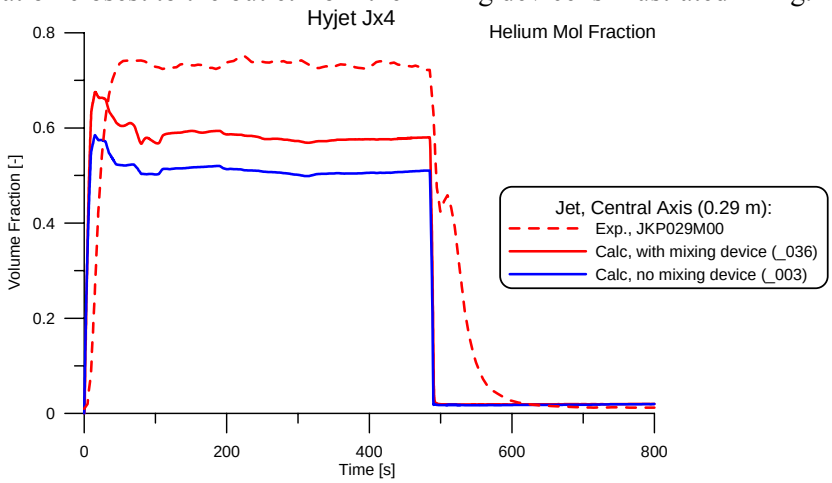

Fig. 6 Improvement of the predicted helium concentration when the mixing device is included in the computational domain (0.29 m above the release opening)

The mesh in the test facility consists mostly of tetrahedral cells. Only in a few locations a combination with hexahedral cells and pyramids was applied. The grid generator Gridgen used here allows creating any combination of structured and unstructured cells. The influence of the mesh type on the results

was not investigated further.

Two examples of the tetrahedral mesh in the jet area of the test facility are shown in Fig. 7. According to the arrangement of measurement probes (Fig. 2) and the theoretical expansion of a jet, very small cells are located in this region. They grow outside of this cone to a standard cell length of about 0.2 m. The total number of cells in the complete test facility is 775619.

The close-up in Fig. 7 provides a cut through the mesh in the mixing chamber and shows the reflecting plate between opening U69 and the gas release device. The gas mixture enters the test facility at the position of the dotted red line included in Fig. 2 which represents the lowest plane modelled from the mixing device in Fig. 7.

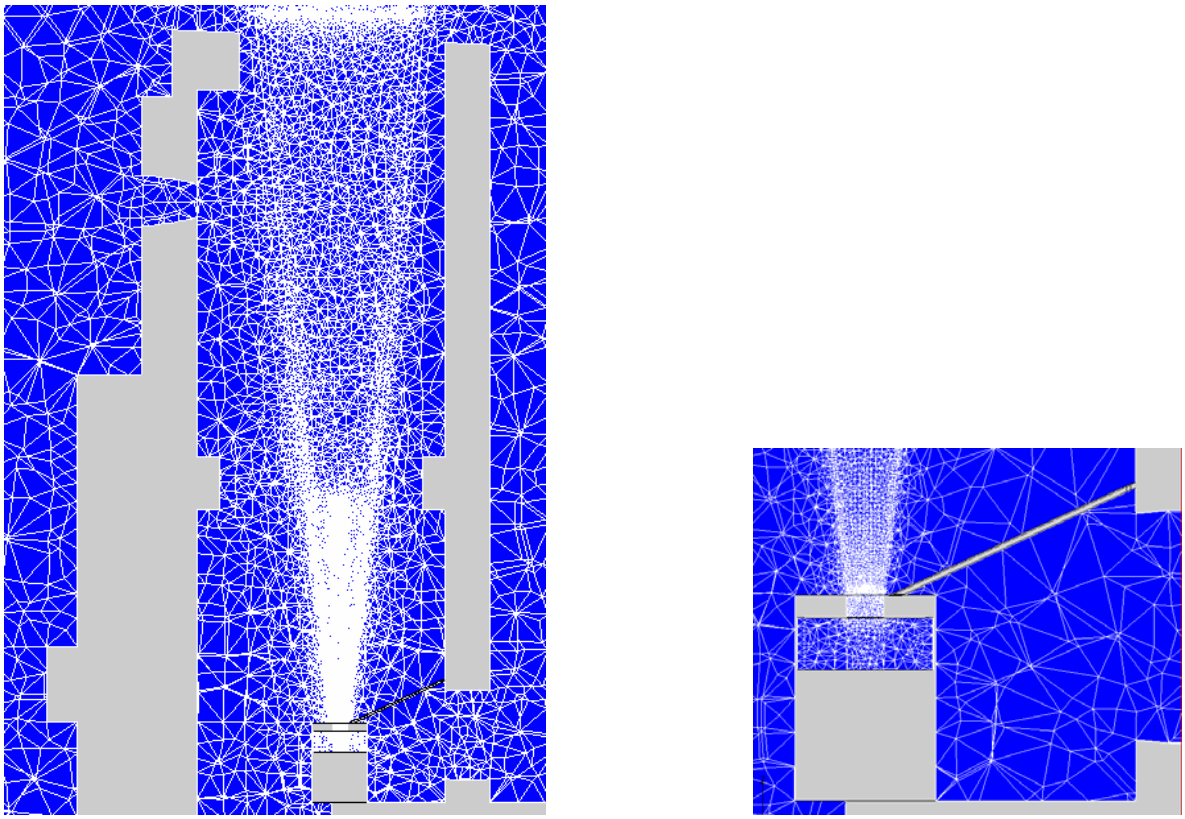

Fig. 7 Cut through the mesh in the jet region and details in the release device

2.2 Initial and Boundary Conditions

The boundary conditions given by the test facility refer to wall temperatures and the flows from the mixing device. The start of the simulations for each experiment coincides with the beginning of the helium injections.

Before the flow mixture enters the test facility it is prepared outside of it as shown in Fig. 8. All measurements like temperatures and mass flows except the mixture temperature are done before the mixing of helium and steam takes place. Helium arrives at about 30 °C and is heated up to the steam temperature. An estimation of the condensation flow required was made. About 8% of the total steam flow may condense in order to heat up helium by about 90 K. But there is more steam necessary to keep the metallic structures of the mixing device at a constant temperature. There is no quantitative information available on this. Even if not considered 8 % less steam flow appears to be the minimum to deduct

to deduct from the measured steam flow. However, some uncertainty remains about the real steam fraction entering the test facility. If less steam would be found in the entering mixture then automatically higher helium fractions in the jet would be measured. Some underestimation of the simulations could be explained in this way.

After steam correction the measured flows from Fig. 4 were directly used as input to the code.

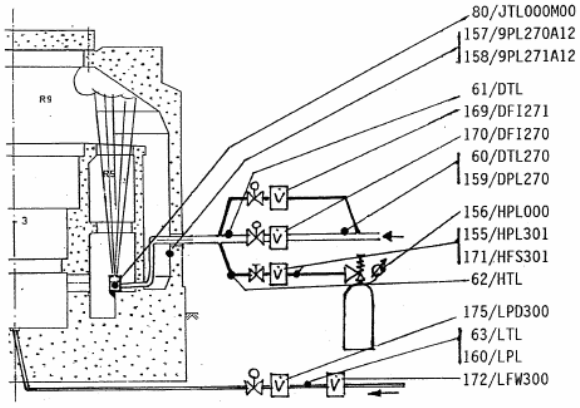

Fig. 8 Set-up of the injected gas mixture

The initial temperature distribution in the BM-C was calculated from the temperature probes at the time the helium injection started. There were not enough temperature probes in the gas space and at walls to get precise information about any location in the BM-C. A three-dimensional interpolation scheme was applied to produce a temperature field across the test facility and along the walls from the available probes. The result is shown in Fig. 9. The wall temperatures can be considered to be constant over the given simulation times as is illustrated on the right side of Fig. 9. The temperatures shown are from experiment Jx4 but the same distribution was observed with test Jx81. The displayed outer wall temperatures from compartment R9 are not monotonic from ceiling to bottom. This is due to the flow field in the test facility which developed during the heating phase prior to each experiment. All walls are treated as boundary condition in the simulations and are not included in the mesh. It turned out that the floor temperatures in all lower compartments were at lower values. This fact is included in the code model as a separate boundary condition for the floor walls based on the measurements available.

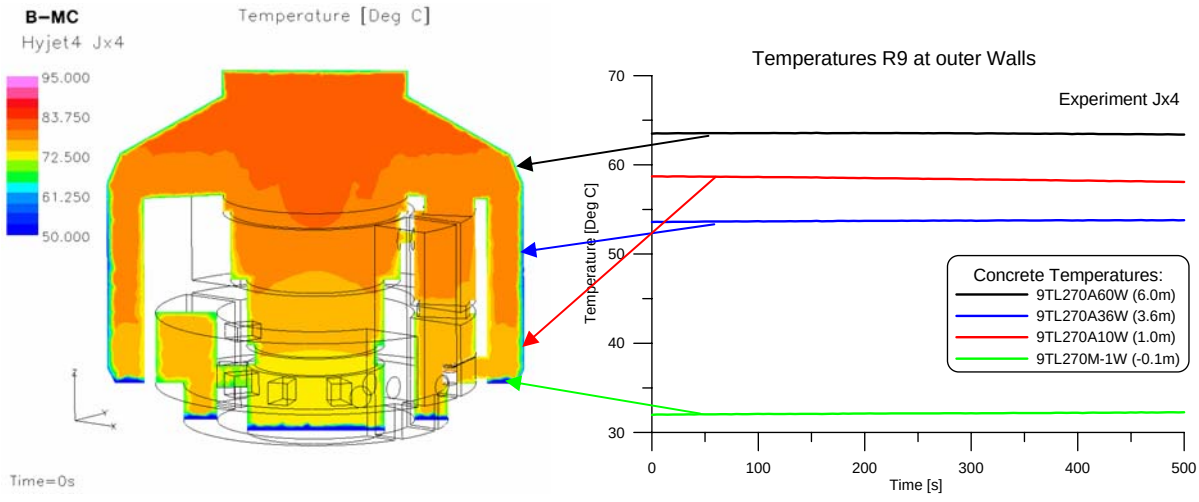

Fig. 9 Initial gas temperature distribution together with selected wall temperatures in the test facility for test Jx4

In CFX all walls are treated as walls at constant temperature with steam condensation allowed on them. The condensation model for bulk and wall condensation is a user supplied model. It has been validated in the SARNET NoE (Network of Excellence) and applied as described by Heitsch (2007).

The simulations used the adaptive time stepping feature of CFX with time steps between 0.05 and 0.5 s. This range of time steps ensured that each time step converged to 10^{-4} of the rooted mean squares of the residuals.

3 SIMULATIONS

All simulations presented here were carried out by the CFX version 10 (Ansys, 2006). As already mentioned the code was extended by bulk and wall condensation models to cope with these important phenomena in containment simulations. A major source of influence on the calculated results is always the turbulence model employed. Therefore three different turbulence models were applied to both experiments. These are the standard k-ε, the RNG k-ε and the SST turbulence models. The RNG k-ε model provided good results in an earlier work (Heitsch, 2000) but with a previous generation of CFX. The SST (shear stress transport) model became popular with the recent versions of CFX and was already applied in a comprehensive containment (Heitsch, 2007). This model should behave close to the k-ε model in free space and like a k-ω model at walls. With the given experiments the most important effects are observed distant from walls; hence k-ε and SST models should predict results very similar to each other. With the slow jet experiment Jx4 the differences in the predictions are smaller than with the fast jet test Jx81. However, predictions are closer to the measurements with experiment Jx81 (when using the RNG k-ε model) than with test Jx4.

The focus of the HYJET experiments was clearly the investigation of jets under various conditions. The presentation of results follows this approach by comparing mainly data from the jet region with numerical results.

3.1 Slow Jet (Jx4)

Results from the slow jet experiment Jx4 are presented here using the RNG k-ε model. Differences to the other turbulence models are discussed later.

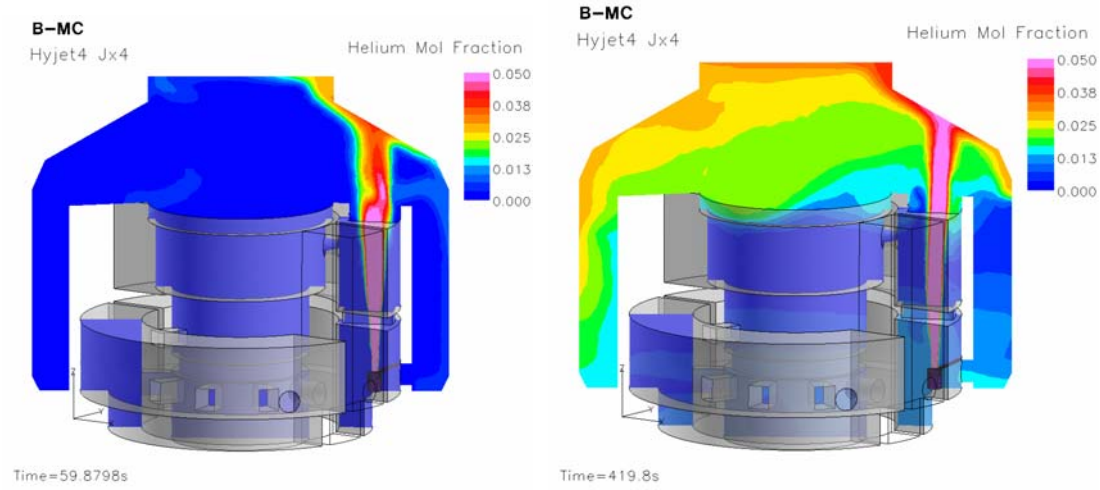

Fig. 10 Evolution of helium molar fraction during test Jx4 (left: 60 s after start of helium injection, right: 420 s after start of injection)

During the injection of helium there is a continuous increase of this gas in the upper part of the facility. The concentrations remain low compared with experiment Jx81 because the total amount of mass fed in is only 1.05 kg. Fig. 10 illustrates the accumulation of helium. This figure represents a vertical

cut through the BM-C touching the central axis of the facility and the injection device. Two situations are shown in the figure: short after the beginning (60 s) and close to the end of injection (420 s). During this time the jet has slightly changed its appearance in the upper section of the facility.

The helium molar fraction along the central axis of the jet varying with time is shown in Fig. 11. The closest probe above the helium-steam exit pipe is found at a distance of 0.29 m (compare right side of Fig. 2 for elevations relative to the outlet opening). In this position the measurement is systematically under-predicted. It was already mentioned that there is a slight uncertainty in the steam fraction which really enters the BM-C. This would directly influence the volumetric fraction of helium. Although the grid is built from very small cells in this region the applied tetrahedral cells in general are more diffusive than hexahedral cells. Another contribution to numerical diffusion may be found in the discretization schemes (although second order accurate was selected).

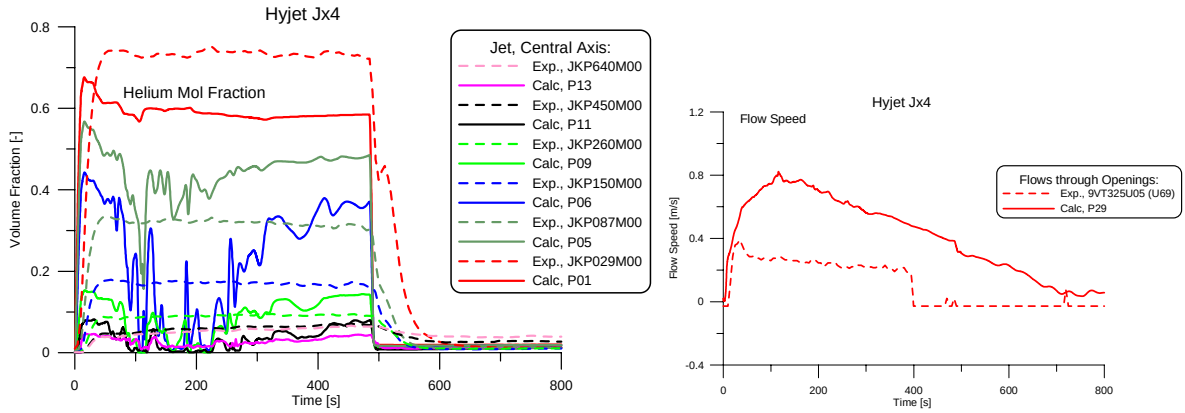

Fig. 11 Prediction of helium concentrations vs. experimental data (dotted lines are experimental data) and flow speed through opening U69

At higher positions there is sometimes an overestimation of the measured data but at position 1.5 m (blue lines) a longer lasting underestimation of the measurements is shown. This observation can be explained by the fact that the jet is oscillating slightly compared with the idealized vertical axis at which the probes are located. The remaining air entrainment through opening U69 causes the jet to move to the opposite position. This is not a stable effect therefore the code calculates oscillations which become remarkable at higher elevations. The flow speed through opening U69 is calculated with a higher value than the measured one. It should be remarked that the calculated and the measured speeds are of different nature. The calculated speed equals to a point value at the central axis of the flow opening whereas the measured speed represents an average over the cross section of the turbine flow meter. Further, it is also possible that the existing walls in the test facility were rough walls compared with the smooth walls assumed in the CFX model. This would create higher flow losses and consequently lower velocities. With the available information it is however not possible to quantify this effect.

3.2 Fast Jet (Jx81)

Experiment Jx81 was carried out with a considerably higher helium injection flow rate than the previous experiment. About 8 times more helium passed through the injection opening.

Although the injection time is shorter for test Jx81 higher helium concentrations are observed than with test Jx4. In Fig. 12, similar to test Jx4, the helium molar fractions at two times of the injection phase (60 s and 200 s) are depicted. In this figure two cuts parallel to the horizontal coordinate axes were drawn. Both cuts run through the injection device. The complex geometry of the BM-C creates non-symmetric cutting planes. It can be seen that the distribution of helium to some locations is very limited and non-uniform. After 200 s there is still almost no helium in some compartments (right side

in Fig. 12) due to missing connections to the other rooms.

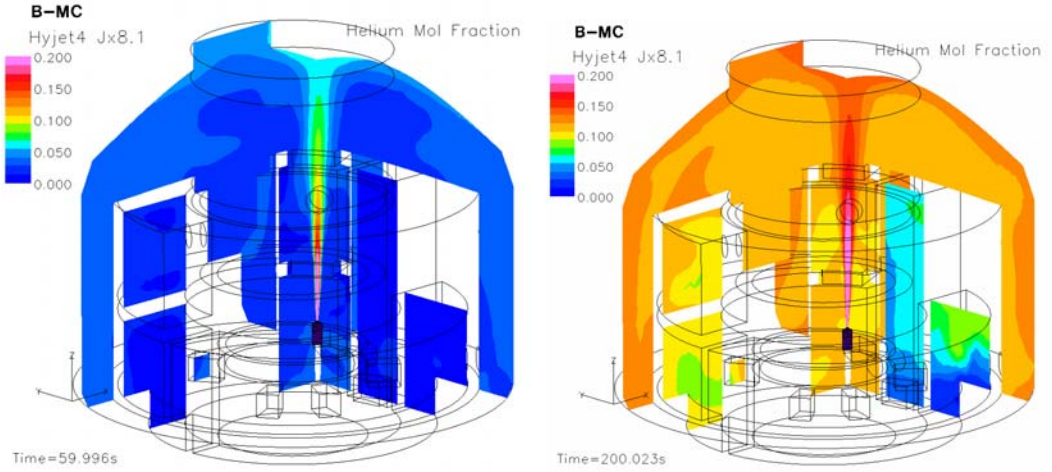

Fig. 12 Helium injection during test Jx81

Fig. 13 reflects similar to Fig. 11 to which degree measurements are met in the central axis of the jet zone. Again the closest probe to the release opening is under-predicted while at some locations above higher-than-measured values are calculated. It is possible that the calculated jet is not always in the same position as the measured was. The calculated oscillations around the central axis of the jet may be triggered by numerical effects and are not predictable.

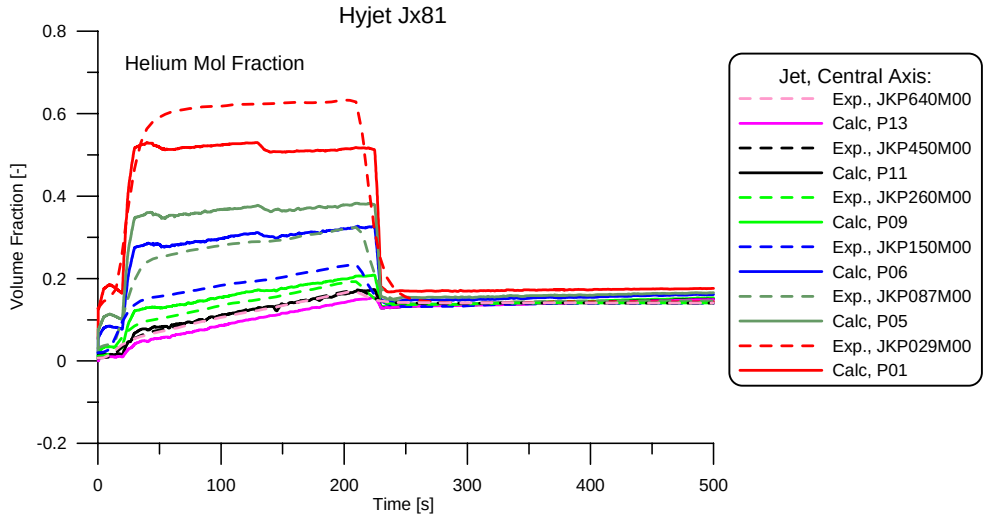

Fig. 13 Helium molar fractions in the jet axis (experiment Jx81)

As Fig. 10 and Fig. 12 imply, in most regions of the test facility helium concentrations grow with increasing time and remain nearly constant after the end of injections. Time histories of molar helium fractions at three selected locations from experiment Jx81 are shown in Fig. 14. There is quite good agreement with the available measurements. The concentration growth is observed with the same gradients for measurement and simulation. But there is at two locations (compartments R5 and R6, blue and green lines) a short delay in the simulation before the first helium appears.

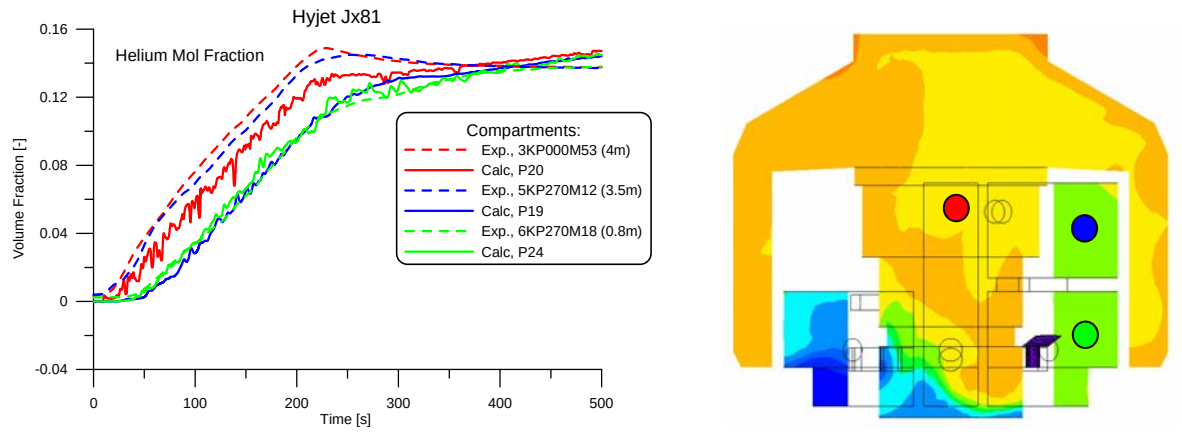

Fig. 14 Samples of helium molar fractions outside of the jet (line colours correspond to locations in test facility)

3.3 Influence of Turbulence Model

An important investigation was made concerning the influence of the turbulence model chosen. As mentioned before three two-equation models were used for each experiment. These are the RNG k-ε, the standard k-ε model and the SST model. Results are depicted in Fig. 15.

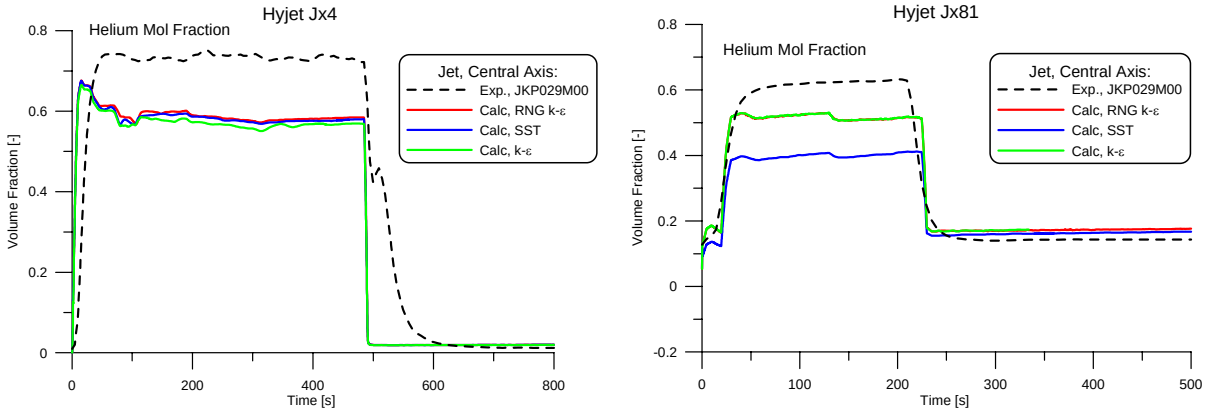

Fig. 15 Influence of the turbulence model on the helium concentration 0.29 m above outlet (left test Jx4, right Jx81)

With both experiments at the closest position from the outlet opening (0.29 m distance) the RNG k-ε model and the standard k-ε model give almost identical (good) results. The SST model predicts a considerably lower value only for test Jx81. For all three models production and dissipations terms due to buoyancy were switched on in the physical setup of the CFX models.

This is not the place to draw conclusions about the applicability of the different turbulence models. At the next higher position the predictions are already more distributed particularly for test Jx4 (earlier dilution of the jet). However, it underlines how important the parallel application of similar turbulence model for jet simulations is. The RNG k-ε model ended up with good results in all simulations carried out.

3.4 Discretization Errors

An additional investigation was carried out to quantify the influence of numerical errors on the simulation results. For this purpose an additional simulation with the upwind discretization scheme in space

and the first order backward Euler scheme in time was carried out. Results for the closest jet probe to the gas release opening are shown in Fig. 16.

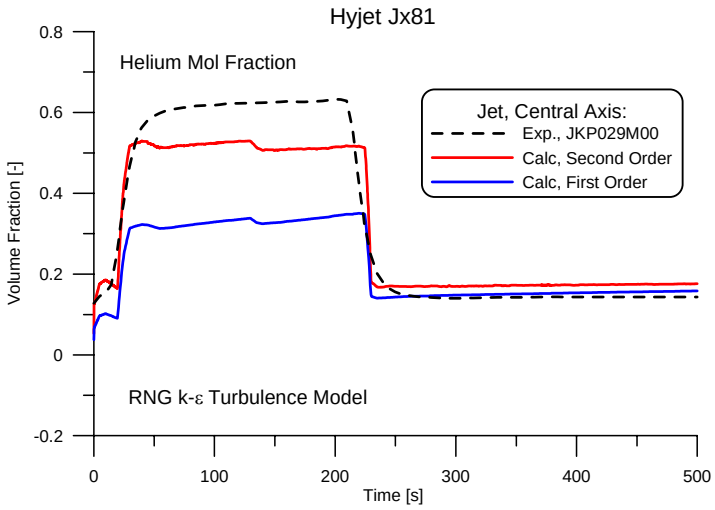

Fig. 16 Influence of the discretization scheme on the jet prediction (test Jx81, 0.29 m)

It turns out that the first order simulation is much more diffusive because the calculated concentration is considerably lower. This implies that there is still a potential for mesh improvement in the simulations, because a coarser mesh involves larger numerical errors once the discretization scheme is changed. As a continuation of the simulations presented in this work a finer grid in the jet region could be created to further investigate the influence of numerical errors. However, in view of an application of equally fine grids in a containment application this approach seems not to be feasible and longer problem times could not be covered.

4 CONCLUSIONS

Simulations on two HYJET experiments in the Battelle Model Containment with CFX were presented and discussed. The HYJET experiments carried out in 1996 were designed as integral tests with the interaction of several phenomena. Due to the size of the test facility, the instrumentation could not cover all quantities (like steam concentrations) or provide probes in a spatial density required for the validation of single phenomena in a CFD code. However, the HYJET experiments are appropriate if the interaction of different types of flows with heat transfer in a realistic geometry is of interest. The HYJET experiments cover a wide range of speeds of either helium or helium-steam jets. An experiment without steam was analysed earlier (Heitsch, 2000). The two experiments analysed in this work include steam condensation to be as realistic as possible. The condensation itself could not be evaluated separately because of lacking measurement information. Condensation acted as a background process and could be quantified.

The experiments selected for simulation are the tests Jx4 and Jx81 with jet release speeds of 4.9 m/s and 730 m/s respectively. These release speeds are representative of a wide range of possible flow conditions in a nuclear containment after a loss-of-coolant accident. Both experiments could be modelled with good or sufficient agreement to the measured data. Emphasis was given to the comparison against data in the jet region. It remains open if model approximations and numerical errors are the only cause of the disagreements because some uncertainties from the experiments exist.

Additional investigations were performed to substantiate the results obtained. In order to quantify model and numerical errors three different turbulence models were applied to each experiment. The

RNG k-ε model turned out to provide predictions for both experiments with the smallest differences to the measured data. The adaptive time stepping mechanism of CFX was applied and saved computing time while ensuring good convergence of all time steps.

REFERENCES

M. Andreani, K. Haller, M. Heitsch, B. Hemström, I. Karppinen, J. Macek, J. Schmid, H. Paillere, H. Toth, *A Benchmark Exercise on the Use of CFD Codes for Containment Issues using Best Practice Guidelines: A Computational Challenge*, OECD CFD4NRS Workshop, Munich, (2006).

ANSYS, CFX-10, Canonsburg Pennsylvania, (2006).

M. Heitsch, *Simulation of Jets and Stratification by CFD*, 8th International Conference on Nuclear Engineering (ICONE8), Paper 8574, Baltimore, (2000).

M. Heitsch, R. Huhtanen, Z. Techy, C. Fry, P. Kostka, J. Niemi, B. Schramm, *Severe Accident Simulation using CFD Codes*, The 12th International Topical Meeting on Nuclear Reactor Thermal Hydraulics (NURETH-12), Paper 108, Pittsburgh, (2007).

T. Kanzleiter, *Anfangs- und Randbedingungen der HYJET Versuche zur Wasserstoff-Verteilung im Freisetzungsstrahl und im Containment*, Report BF-R40.075-31, Eschborn Germany, (1995).

T. Kanzleiter, H. Holzbauer, K. Fischer, M. Geiß, W. Häfner, *HYJET-PACOS Versuche im Modellcontainment*, Final Report BF-R40.075-01, Eschborn Germany, (1996).

H. Wilkening, D. Baraldi, M. Heitsch, *CFD simulations of light gas release and mixing in the Battelle Model-Containment with CFX*, Nuclear Engineering and Design, 238, 618-626 (2008).

ACKNOWLEDGEMENT

Thanks to Dr. Teja Kanzleiter and his team from Becker Technologies for carrying out the HYJET experiments.

Data of the HYJET experiments were provided by the German Federal Ministry of Economics and Technology (BMWi).